JOURNAL OF VIROLOGY, July 1993, p. 3786–3797
0022-538X/93/073786-12$02.00/0
Copyright © 1993, American Society for Microbiology
Vol. 67, No. 7

Specific Pseudorabies Virus Infection of the Rat Visual System Requires both gI and gp63 Glycoproteins

M. E. WHEALY,[1] J. P. CARD,[2] A. K. ROBBINS,[3] J. R. DUBIN,[1] H.-J. RZIHA,[4] AND L. W. ENQUIST[1]*

DuPont Merck Pharmaceutical Company, Wilmington, Delaware 19880-0328[1]; Department of Behavioral Neuroscience, University of Pittsburgh, Pittsburgh, Pennsylvania 15260[2]; Tularik, Inc., South San Francisco, California 94080[3]; and Bundesforschungsanstalt für Viruskrankheiten der Tiere, D-7400 Tubingen, Germany[4]

Received 23 December 1992/Accepted 15 March 1993

Transneuronal transport of pseudorabies virus (PRV) from the retina to visual centers that mediate visual discrimination and reflexes requires specific genes in the unique short region of the PRV genome. In contrast, these same viral genes are not required to infect retinorecipient areas of the brain involved in circadian rhythm regulation. In this report, we demonstrate that viral mutants carrying defined deletions of the genes encoding glycoprotein gI or gp63, or both, result in the same dramatic transport defect. Efficient export of either gI or gp63 from the endoplasmic reticulum to the Golgi apparatus in a fibroblast cell line requires the presence of both proteins. We also show that gI and gp63 physically interact, as demonstrated by pulse-chase and sucrose gradient sedimentation experiments. Complex formation is rapid compared with homodimerization of PRV glycoprotein gII. We suggest that gI and gp63 function in concert to affect neurotropism in the rat visual circuitry and that a heterodimer is likely to be the unit of function.

Pseudorabies virus (PRV) is an alphaherpesvirus that causes economically significant disease in swine (2, 32, 33, 35, 45). PRV has a predilection to infect neurons, particularly sensory neurons, which often results in the establishment of latency in these neurons. Infection of the central nervous system (CNS) generally results in a lytic or productive infection. It is clear from analyses in rodent models that invasion of the CNS from the periphery by PRV occurs in an ordered fashion in which the virus is contained within synaptically linked neurons (4, 6, 15, 25, 31, 37, 38, 42, 43).

To further understand these events, our laboratory has studied the transneuronal transport of PRV in the rat visual system (5, 6). Retinal ganglion cells project through the optic nerves and terminate in a number of functionally distinct regions of the central neuraxis. PRV infects ganglion cell bodies in the retina, replicates in these cells, and is subsequently transported via anterograde mechanisms to axon terminals that synapse on these retinorecipient neurons in the CNS (5, 6). We have characterized the infectivity of several PRV variants in this system and have shown that the virulent strain, PRV Becker (PRV-Be), is transported to all known projections of the retinal ganglion cells in the CNS, while the attenuated strain, PRV Bartha (PRV-Ba), is predominantly transported to neural centers involved in the regulation of circadian rhythms (6). Subsequently, we demonstrated that a deletion of the gI gene in PRV-Be resulted in an identical restricted neurotropism as PRV-Ba (5).

In this report, we demonstrate that a second PRV glycoprotein (gp63) plays a significant role in the restricted neurotropism phenotype. Specifically, isogenic strains of PRV-Be lacking the gI gene, the gp63 gene, or both genes exhibit identical phenotypes after infection of the rat retina. Since previous work suggested that gI and gp63 could be immunoprecipitated as a complex from infected cells (48), we examined the interactions of these two glycoproteins in more detail. We demonstrate unequivocally that the two proteins form a physical complex within minutes after synthesis in the endoplasmic reticulum (ER). Moreover, this interaction is required for the efficient export of either glycoprotein from the ER to the Golgi apparatus. The complex of gI and gp63 is found in the mature virus envelope.

Thus, even though gI and gp63 are classified as nonessential for growth in cultured cell lines (2, 21, 23, 29, 32, 33, 45), they are required to infect specific classes of neurons in the rat retina. Furthermore, our results are consistent with the hypothesis that the unit of function for this interaction is a complex of gI and gp63.

MATERIALS AND METHODS

Cells and viruses. PK15 cells (swine kidney cells) were used to propagate all PRV strains. PRV-Be (virulent) and PRV-Ba (attenuated) have been described previously (1, 4). PRV91, PRV98, and PRV99 are isogenic strains with specific deletions of gI, gp63, and both gI and gp63, respectively, in the PRV-Be background (Fig. 1). PRV91 has been described previously (5). PRV98 was derived from pALM98, which was constructed in the following manner. A 6.1-kb *Pst*I-*Mlu*I fragment from the PRV-Be *Bam*HI-7 fragment was cloned into the *Pst*I-*Mlu*I sites of pGEM5Zf+ (Promega). This plasmid was designated pALM93. pALM93 was subsequently digested with *Csp*I, and a linker that contained both a *Bsp*EI and an *Xcm*I site was inserted. This plasmid was designated pALM96. pALM96 was digested with *Xcm*I, and the resulting 8.1-kb fragment was religated and transformed into NF1829. The resulting clone has a deletion extending from 28 bp upstream of the ATG codon of the gp63 gene to 1 bp before the TGA stop codon of the coding region. This clone was designated pALM98. PRV99 was derived from pALM99. To construct pALM99, pALM96 was digested with *Bsp*EI, and the 6.3-kb fragment was religated and transformed into NF1829. This results in a deletion extending from 28 bp upstream of the ATG of the gp63 gene to 75 bp upstream of the TAA stop codon of the gI gene. This plasmid was designated pALM99.

For construction of a viral recombinant carrying the gp63

---

* Corresponding author.

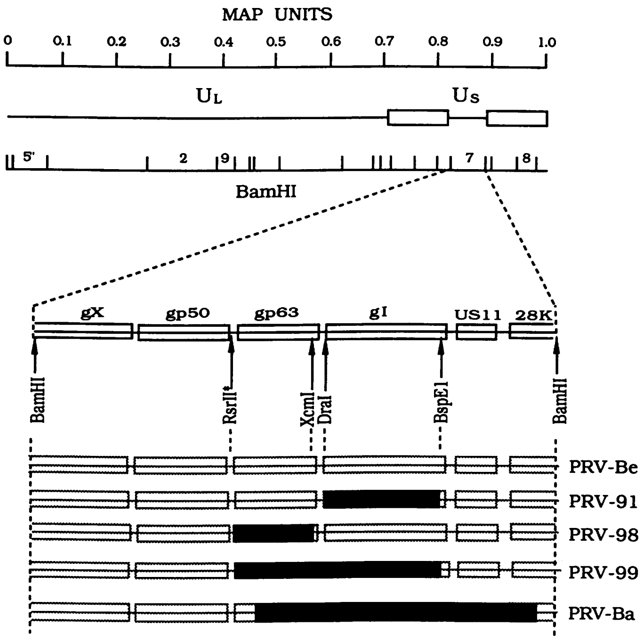

FIG. 1. PRV genome and map of the relevant mutations. The PRV genome is indicated on the second line, with the map units above and the *Bam*HI restriction map below (2). The *Bam*HI-7 fragment from the unique short (U_S) region is expanded, and the genes are noted on the fourth line (31). Deletions in the isogenic PRV-Be mutants are indicated by the extents of the black boxes. The deletion in PRV-Ba is indicated on the last line. Relevant restriction sites are indicated. The *Rsr*II* site was modified by insertion of a linker containing an *Xcm*I and *Bsp*EI sites. The PRV91 deletion is from *Dra*I to *Bsp*EI, the PRV98 deletion is from *Rsr*II* (*Xcm*I) to *Xcm*I, and the PRV99 deletion is from *Rsr*II* (*Bsp*EI) to *Bsp*EI. U_L, unique long region.

deletion, pALM98 plasmid DNA was cotransfected with PRV91 viral DNA. Plaques were screened with a gI monoclonal antibody in an immunoassay, and plaques reactive with the gI antibody were purified several times. This resulting virus was designated PRV98. For construction of a viral recombinant lacking both gI and gp63, pALM99 plasmid DNA was cotransfected with PRV-Be DNA. Resulting progeny were screened in an immunoassay with a monoclonal antibody to gI, and plaques which were nonreactive were purified and designated PRV99.

Antisera. Rabbit polyclonal antiserum Rb134 (4) recognizes virus glycoproteins as well as virus capsid proteins. Goat polyvalent antiserum 282 (39) recognizes the gIII glycoprotein. Four gI monoclonal antibodies were used in these experiments. Three of the antibodies, M133, M156, and M138, were a kind gift from Tamar Ben Porat. These antibodies react with complexed and uncomplexed gI and were used as a pool in 1:1:1 ratio. The remaining gI monoclonal antibody, 1/14 (12), reacts strongly with gI when complexed with gp63 and poorly with uncomplexed gI. The polyvalent rabbit antiserum Rb1544 recognizes the glycosylated precursor of the gp63 glycoprotein but not the glycosylated mature species. This antibody was produced by immunizing rabbits with a polypeptide corresponding to amino acids 60 to 268 of the gp63 protein expressed in *Escherichia coli*. The polyvalent rabbit antiserum Rb1544+ is a later serum sample from the rabbit that produced antiserum Rb1544. This antiserum retains strong reactivity with the gp63 precursor but also exhibits weak reactivity with the mature form of gp63. A brief description of these antibodies is also provided in Table 1.

TABLE 1. Properties of antibodies used

Antibody	Specificity	Species immunoprecipitated
gI pool	gI-specific monoclonal mix	All forms of gI[a]
Rb1544	gp63-specific polyvalent	Precursor but not mature form of gp63
Rb1544+	gp63-specific polyvalent	Like Rb1544, but weak reaction with mature polyvalent form of gp63
282	gIII-specific polyvalent	All forms of glycoprotein gIII
Rb134	PRV-specific polyclonal	Virus glycoproteins as well virus capsid proteins

[a] A notable exception is that this pool does not recognize the gI protein made after 2 min of labeling with radioactive cysteine. It is likely that the epitopes recognized by this pool are not yet formed in this short labeling period (see Fig. 6).

Pulse-chase analysis. The pulse-chase procedure was described previously (39). Briefly, PK15 cells were infected at a multiplicity of infection (MOI) of 10 with PRV-Be, PRV91, or PRV98. For the complementation pulse-chase experiments, PK15 cells were infected with PRV91 or PRV98 at an MOI of 10 or PRV91 and PRV98 at an MOI of 10 each (total MOI of 20). At 5.5 h postinfection, the cells were starved for cysteine. At 6 h postinfection, a radioactive pulse containing 200 μCi of [^{35}S]cysteine per ml was administered for 2 min. Following the pulse, the radiolabel was removed, and the cells were incubated in medium containing excess nonradioactive cysteine for various times (chase). At the desired chase times, the monolayers were harvested and the samples were immunoprecipitated.

Sedimentation in sucrose gradients. Sedimentation in sucrose gradients was done essentially as described by Hampl et al. (14) and Sarmiento and Spear (40), with minor modifications. Briefly, PK15 monolayers were infected and subjected to the pulse-chase protocol described above. At various times, the infected cells were solubilized in 1% Triton X-100–150 mM NaCl–50 mM Tris (pH 7.5) on ice for 10 min. Next, samples were scraped into tubes, and the nuclei were pelleted at 11,750 × *g* for 5 min at 4°C. Supernatants were layered onto an 11-ml 5 to 15% sucrose gradient containing 0.1% Triton X-100, 150 mM NaCl, and 50 mM Tris (pH 7.5) and sedimented in an SW41 rotor at 196,000 × *g* for 20 h at 4°C. Fractions from each gradient were used for immunoprecipitation.

Polyacrylamide gel analysis. All immunoprecipitates were loaded onto sodium dodecyl sulfate (SDS)–10% polyacrylamide gels. Fluorography was conducted with sodium salicylate (8) and was followed by autoradiography.

Animals and experimental paradigm. A total of 50 adult male Sprague-Dawley rats, weighing 200 to 350 g at the time of sacrifice, were used in these analyses. Food and water were freely available throughout the course of each experiment, and the photoperiod was standardized to 14 h of light and 10 h of dark (light on at 0600 h). Experimental protocols were approved by the Animal Welfare Committee and were consistent with the regulations of the American Association for Accreditation of Laboratory Animal Care and those in the Animal Welfare Act (Public Law 99-198). All animals were confined to a biosafety level 2 laboratory throughout the course of each experiment; specific safeguards necessary

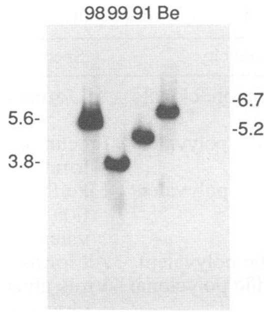

FIG. 2. Southern blot analysis of nucleocapsid DNA extracted from PRV-Be (Be), PRV91 (91), PRV98 (98), and PRV99 (99). Nucleocapsid DNA was digested with *Bam*HI, and the resulting fragments were resolved in a 1% agarose gel and blotted onto nitrocellulose. The membrane was hybridized with ^{32}P-labeled *Bam*HI-7 fragment and prepared for autoradiography. Sizes of the *Bam*HI-7 fragments of PRV98 (5.6 kb) and PRV99 (3.8 kb) are indicated at the left; sizes of PRV-Be (6.7 kb) and PRV91 (5.2 kb) are indicated at the right.

for operation of this laboratory have been noted by Card et al. (4).

The procedures for infection of the rat retina and subsequent immunohistochemical analyses have been described by Card et al. (6). Coronal sections were reacted with various PRV-specific antisera, and antigen in the tissue was localized with the avidin-biotin modification of Sternberger's immunoperoxidase procedure (41).

RESULTS

Rationale. Our laboratory has described a profound difference in the neurotropism exhibited by PRV-Be (virulent) compared with PRV-Ba (attenuated) after in vivo infection of rat retinal ganglion cells (6). We further demonstrated that deletion of the gI gene from strain PRV-Be resulted in the PRV-Ba neurotropism phenotype (5). However, Card et al. (5) noted that while the gI gene product was necessary, it might not be sufficient to infect all retinorecipient areas of the CNS. It was known that in tissue culture infections, gI interacted with gp63, another PRV glycoprotein, and that the complex could be immunoprecipitated with antibodies to either glycoprotein (48). Furthermore, all known homologs of gI in the alphaherpesvirus group form similar complexes with gp63 homologs (9, 16, 17, 20, 46). In this report, we use in vivo and in vitro experiments to test the hypothesis that gI and gp63 function as a complex.

Construction of isogenic PRV strains. We constructed isogenic strains of PRV-Be containing defined deletions of the gI and/or gp63 genes, as described in Materials and Methods and shown in Fig. 1. PRV-Ba contains other mutations not depicted in this schematic drawing (21, 23, 29, 32, 34). The presence of the desired deletion in each recombinant virus was demonstrated by restriction enzyme digestion and DNA hybridization. A typical result is shown in Fig. 2. The probe used for this analysis was a *Bam*HI-7 fragment which was nick translated with [^{32}P]dCTP. The data show that the viruses contain the anticipated deletions and that there are no other obvious rearrangements within this region of the genome. For our experiments, it was critical to show that deletion of the gI gene did not affect expression of gp63 and vice versa. RNA was extracted from cells infected with each mutant virus, and the pattern of gI- and gp63-specific RNA was determined by Northern (RNA) blot analysis. PRV91 (gI$^-$ gp63$^+$) and PRV98 (gI$^+$ gp63$^-$) had the expected RNA profiles for gp63 and gI transcripts, respectively (data not shown).

Expression of gI and gp63 antigens in the rat hypothalamus after infection of the retina with PRV. To verify that the mutants described above expressed the appropriate glycoproteins in vivo, we used immunohistochemical methods to identify specific viral antigens in infected brain tissue. The vitreous body of the eye was infected with one of the four strains of PRV, i.e., PRV-Be, PRV91, PRV98, or PRV99. Subsequently animals were sacrificed at the times indicated in Fig. 3. The brains were fixed and sectioned as described in Materials and Methods. The area of the hypothalamus containing the suprachiasmatic nucleus (SCN), a cell group involved in circadian rhythm regulation, was examined for specific immunoreactivity (Fig. 3). Each column represents an adjacent serial section reacted with a different antiserum. Figure 3A, D, G, and J were reacted with Rb134 serum that identifies most major structural antigens of PRV; Fig. 3B, E, H, and K were reacted with gI-specific monoclonal antibody 1/14; and Fig. 3C, F, I, and L were reacted with gp63 precursor-specific antiserum RB1544. The SCN infected with all viruses demonstrated strong immunoreactivity with Rb134 serum; PRV91 expressed gp63 but not gI, PRV98 expressed gI but not gp63, and PRV99 expressed neither gI nor gp63.

Differential patterns of viral mutant infectivity of the rat visual system. Retinal ganglion cells project through the optic nerves to terminate in a number of functionally distinct regions of the central neuraxis (5, 6). A diagram depicting the central visual projection system and the different patterns of infectivity resulting from intraocular injection of virulent (PRV-Be) and attenuated (PRV-Ba) strains is shown in Fig. 4.

The pattern of transport for each mutant virus was analyzed as described in Materials and Methods. The results of the immunohistochemistry analysis in specific regions of the brain are shown in Fig. 5. The top row shows the patterns of staining observed with PRV-Be within the SCN (Fig. 5A), within the lateral geniculate nucleus (Fig. 5B), and within the optic tectum (Fig. 5C). The second row emphasizes the restricted neurotropism of PRV-Ba; viral antigens were detectable only in the SCN (Fig. 5D), and the intergeniculate leaflet (Fig. 5E), not in the dorsal or ventral geniculate nucleus (Fig. 5E) or the optic tectum (Fig. 5F). As described

FIG. 3. Antiserum specificity and glycoprotein expression phenotypes in infected rat brain. Sections shown are through the same plane of the forebrain containing the SCN. All photos were taken at the same magnification and light settings. In each case, serial adjacent sections from infected animals were reacted with antisera generated against purified virus particles (Rb134; left column), gI (middle column), or gp63 precursor (right column). Each horizontal row illustrates a series of sections taken from an animal infected with a different strain of PRV. PRV-Be is shown is the top row, PRV91 is shown in the second row, PRV98 is shown in the third row, and PRV99 is shown in the bottom row. Note that the gI antiserum shows no detectable immunoreactivity in the animals infected with PRV91 or PRV99, whereas the gp63 antiserum was ineffective in the animals infected with PRV98 or PRV99.

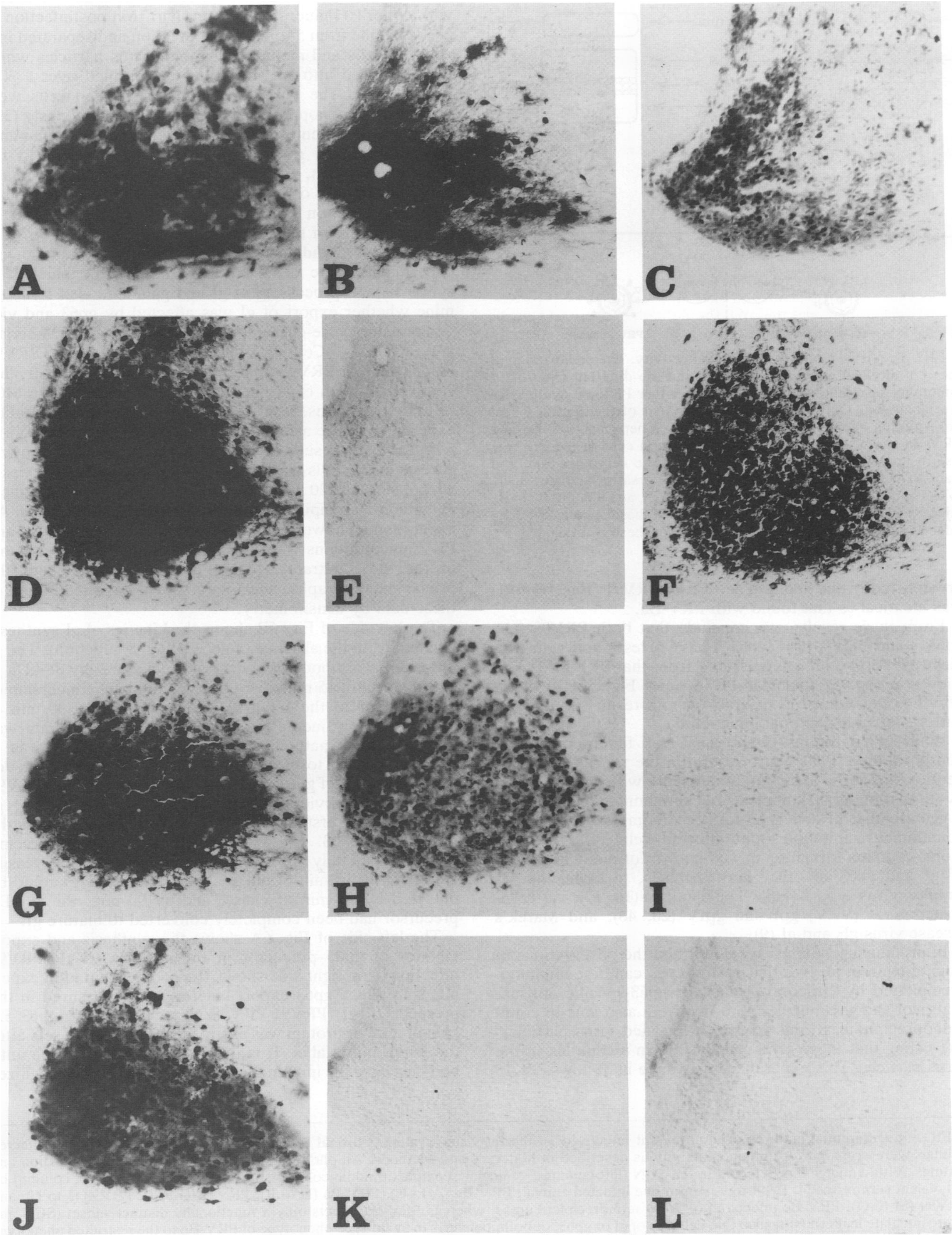
A
B
C
D
E
F
G
H
I
J
K
L

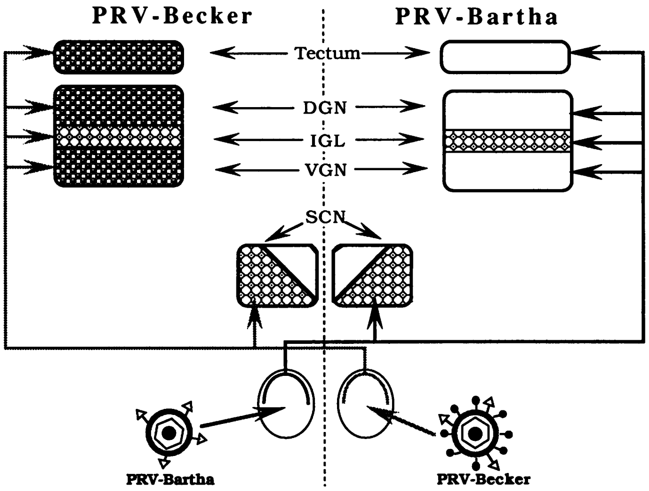

FIG. 4. Visual circuitry and viral infectivity. The organization of the central visual projection systems and the different patterns of infectivity resulting from infection with either PRV-Be or PRV-Ba are illustrated. Only the crossed component of the central visual projection is shown so that the differences between PRV-Be and PRV-Ba can be represented. Retinal ganglion cells in the eye give rise to processes projecting through the optic nerve, chiasm, and tract to innervate the SCN, ventral and dorsal geniculate nuclei (VGN and DGN), intergeniculate leaflet (IGL), and tectum. PRV-Be injected intraocularly infects neurons is all of these regions. PRV-Ba infects only a functionally distinct subset of these neurons.

previously (5), the staining pattern of PRV91 (Fig. 5G to I) was identical to that found with PRV-Ba.

From these results, we conclude that both PRV98 (gI^{+} gp63^{-}) and PRV99 (gI^{-} gp63^{-}) have a restricted neurotropism phenotype indistinguishable from that of PRV-Ba (as shown in Fig. 5J to L for PRV98 and Fig. 5M to O for PRV99). Deletion of gI or gp63 or both results in identical patterns of transneuronal infection.

While glycoproteins gI and gp63 may function independently to affect PRV neurotropism in the rat retina, precedent exists for the idea that gI may work with gp63, perhaps by formation of a complex. Zuckermann and coworkers suggested that gI and gp63 formed a complex detected by coimmunoprecipitation from infected cells (48). Furthermore, complex formation is well known for many homologs of gI and gp63 in other herpesviruses, including herpes simplex virus type 1 (HSV-1) gE and gI (16, 17), varicella-zoster virus (VZV) gpI and gpIV (20, 46), and Marek's disease virus gE and gI (9).

In preliminary studies, we confirmed the observations of Zuckermann et al. (48) that gI and gp63 can be coimmunoprecipitated by either gI-specific or gp63-specific antisera (data not shown). Furthermore, we were also able to coimmunoprecipitate gI and gp63 from purified virus particles, suggesting that these glycoproteins are in a complex in the virus particle. This experiment was done as follows. PK15 cells were infected with PRV-Be at an MOI of 10 and labeled with either [^{3}H]glucosamine from 1 to 16 h postinfection or [^{35}S]cysteine from 5 to 16 h postinfection and separated into infected cells and medium fractions. Virus particles which were released into the medium were purified over a 30% sucrose pad. The virus particles and infected cells were lysed and immunoprecipitated as described previously (39). In these experiments, the gI monoclonal antibody immunoprecipitated both gI and gp63 (data not shown). In the following sections, we extend these basic observations and study the kinetics of complex formation, the requirement of complex formation for proper export of each protein, and the physical nature of the complex.

Kinetics of gI and gp63 synthesis and export. The following experiments were designed to determine the kinetics of synthesis and processing of gI and gp63 and also to determine whether export of gI was affected by gp63 and vice versa, using pulse-chase analyses as described in Materials and Methods. Cells were infected either with PRV91 (gp63^{+} gI^{-}) or PRV98 (gp63^{-} gI^{+}) at an MOI of 10 or, in a complementation experiment, with both viruses at an MOI of 10 for each virus. It should be noted that complementation experiments were also done with an MOI of 5 for each virus with the same results as shown in Fig. 6 (data not shown). After 6 h, the cells were pulse-labeled and chased for 0, 15, 30, 60, 90, and 120 min. The cells were then lysed, clarified, and immunoprecipitated with the appropriate antibodies. All experiments shown in Fig. 6 were done concurrently, and PRV glycoproteins were immunoprecipitated from aliquots of the same extracts. Figure 6 shows examples of the primary fluorographs, and Fig. 7 shows the quantitation of these data by densitometry.

The left side of Fig. 6B shows the kinetics of gI synthesis and export in the absence of gp63 (PRV98 infection). The gI monoclonal antibody pool did not precipitate any 88-kDa gI precursor until 15 min. We observed minimal conversion of gI precursor to the 110-kDa mature form after 90 min of chase. Only by increasing the chase time to 120 min was some 110-kDa mature gI precipitated. This result was in marked contrast to the normally efficient gI export kinetics in the presence of gp63 (right side of Fig. 6B, PRV91-PRV98 coinfection). Obviously, both the rate and extent of gI precursor conversion to mature gI were increased in the presence of gp63. The gI precursor again was not precipitated immediately after the 2-min pulse but was easily identified by 15 min of chase. Mature 110-kDa gI could be detected by 30 min of chase, and by 90 min, the 88-kDa precursor had been completely converted to mature gI.

The left side of Fig. 6A shows the synthesis and export kinetics of gp63 precursor in the absence of gI (PRV91 infection); the right side shows the complementation experiment in which gp63 export kinetics were measured in the presence of gI (PRV91-PRV98 coinfection). The gp63 52-kDa precursor protein was easily identified in both sets after the 2-min pulse-label. It is important to note that the antibody used for the immunoprecipitations, Rb1544, recognizes

FIG. 5. Differential patterns of viral mutant infectivity of the rat visual system. Coronal sections of brains from intraocularly infected animals were prepared for immunoreactivity as described in Materials and Methods. All photos were taken at the same magnification and settings. Viral antigen was detected in the SCN (left column), geniculate complex (middle column), and the optic tectum (right column) by polyvalent serum Rb134. Each row is from one infected animal: PRV-Be (A to C), PRV-Ba (D to F), PRV91 (G to I), PRV98 (J to L), and PRV99 (M to O). PRV-Be infects all of these retinorecipient areas, whereas PRV-Ba infects only a functionally distinct subset (SCN and intergeniculate leaflet). Note also that deletion of gI or gp63, or both, converts the wild-type phenotype of PRV-Be to the restricted phenotype of PRV-Ba.

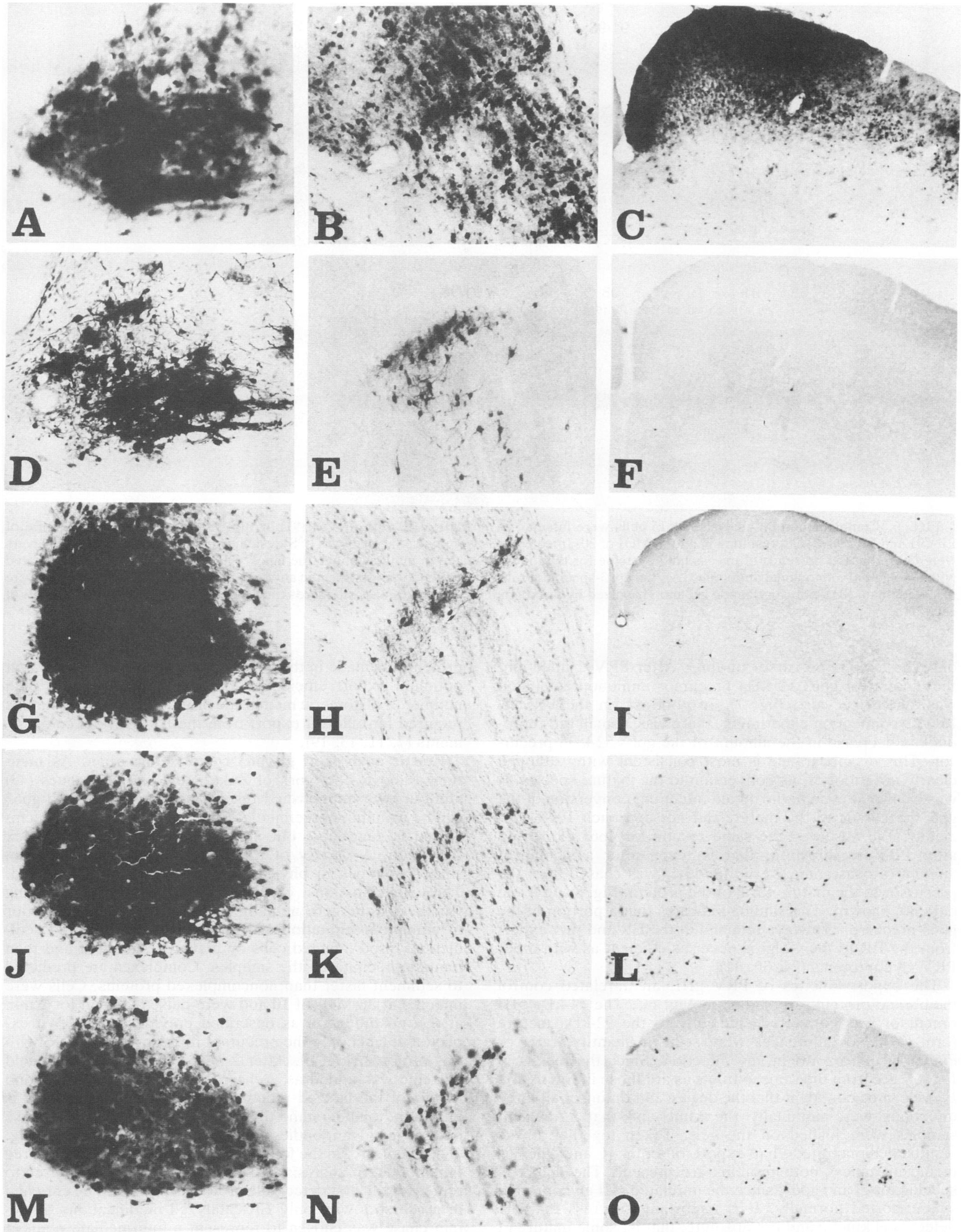
A
B
C
D
E
F
G
H
I
J
K
L
M
N
O

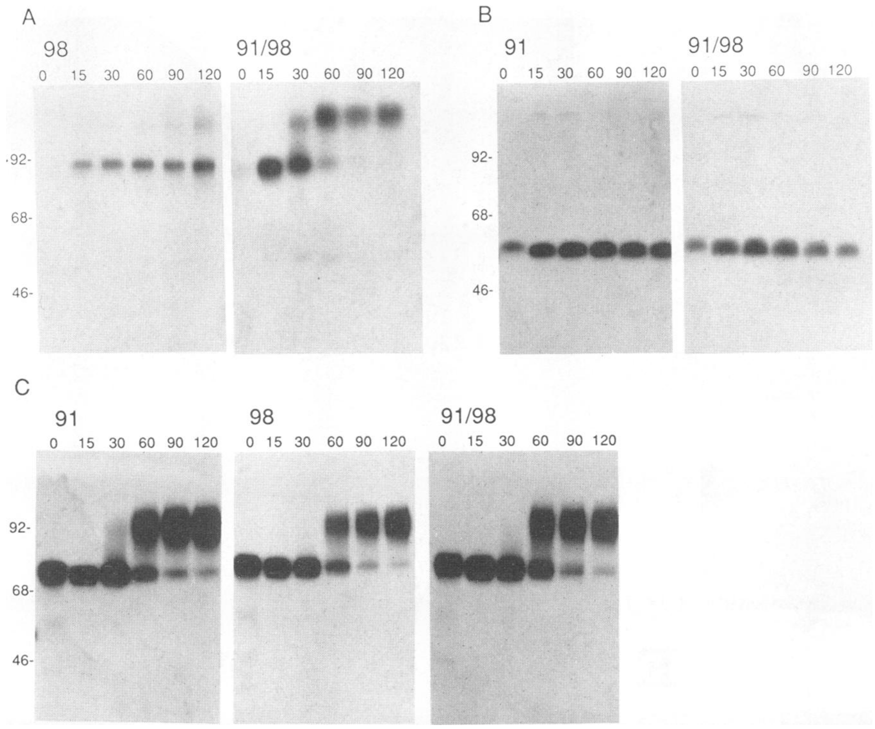

FIG. 6. Complementation analysis. PK15 cells were infected at an MOI of 10 with PRV91 (91) or PRV98 (98) or with a 1:1 mixture of PRV91 and PRV98 (91/98) resulting in a total MOI of 20. Infected cells were pulse-labeled with [^{35}S]cysteine at 6 h postinfection. Monolayers were chased in the presence of excess cold cysteine for the times indicated in minutes above the lanes. Samples were immunoprecipitated with a pool of gI monoclonal antibodies (A), the gp63-specific serum Rb1544 (B), or a gIII-specific antibody 282 (C). Immunoprecipitates were resolved on an SDS-polyacrylamide gel and visualized by fluorography. Molecular mass standards (in kilodaltons) are indicated at the left of each panel.

only the 52-kDa precursor of gp63. After PRV91 infection, the amount of gp63 52 kDa precursor immunoprecipitated was stable (see also Fig. 7). In contrast, in the PRV91-PRV98 coinfection experiment, there was a small but reproducible decrease in the amount of the gp63 52-kDa precursor. This disappearance is most consistent with, although clearly not proof of, its conversion to the mature species. It was clear that even in the mixed infection, conversion of the gp63 precursor to the mature did not approach 100% efficiency. We observed the same results for gp63 expressed after PRV-Be infection; that is, even after a significant amount of chase time, very little gp63 was chased from the precursor to the mature form of the protein (Fig. 8 and 9 and data not shown). This finding indicates that a portion of the gp63 precursor is always retained in the ER and that export from the ER to the Golgi is never as efficient as with other PRV glycoproteins (24, 39, 44).

The export kinetics of PRV gIII, an unrelated control membrane protein, are shown in Fig. 6C. The 74-kDa gIII precursor was converted efficiently to the 92-kDa mature form (39). No differences were seen in quantity, rate, or extent of gIII export in any infection. Since the results in Fig. 6C are from the same extracts as are those in Fig. A and B, we can be confident that the degree and timing of all three infections were nominally the same and that equivalent samples were loaded on the gels. Taken together, these results demonstrated that export of both gI and gp63 is inefficient unless both proteins are present. The defect is specific for gI and gp63, since the unrelated gIII glycoprotein was exported normally. It is important to stress that the defect was kinetic and not absolute; that is, some mature gI protein was made in the absence of gp63 and vice versa, but optimum export efficiency required both proteins. For a number of oligomeric membrane proteins, oligomerization is required for efficient export from the ER to Golgi compartments (7, 11, 13, 19).

Kinetic analysis of gI-gp63 complex formation. As mentioned above, the work of Zukermann and colleagues (48) and our own unpublished results indicate that gI and gp63 can be coimmunoprecipitated from infected cells. Coprecipitation is suggestive but not proof of functional complex formation. A variety of trivial explanations ranging from shared epitopes to physical trapping must be considered. These explanations can be eliminated by determining whether gI and gp63 actually assemble into oligomers prior to immunoprecipitation. To accomplish this, we first sedimented lysed infected cells on a sucrose gradient and then immunoprecipitated the samples. Complexes are predicted to sediment faster than noncomplexed proteins. Cells were infected at an MOI of 10 and were pulsed-labeled for 2 min at 6 h postinfection as described previously (44). We expected to label only the precursor forms of gI and gp63 with this protocol (Fig. 6). After 2 min of labeling, excess cold cysteine was added as a chase so that the processing and export of the labeled precursors could be monitored. It is important to understand that it takes at least 10 min of chase before our gI antibodies immunoprecipitate anything (Fig. 6B). Therefore, in the following experiments, we chose three time points for analysis. A 10-min chase sample was used to represent the first detectable proteins and should be enriched in precursors with only ER-catalyzed modifications. A 60-min chase was chosen to represent a intermediate point at

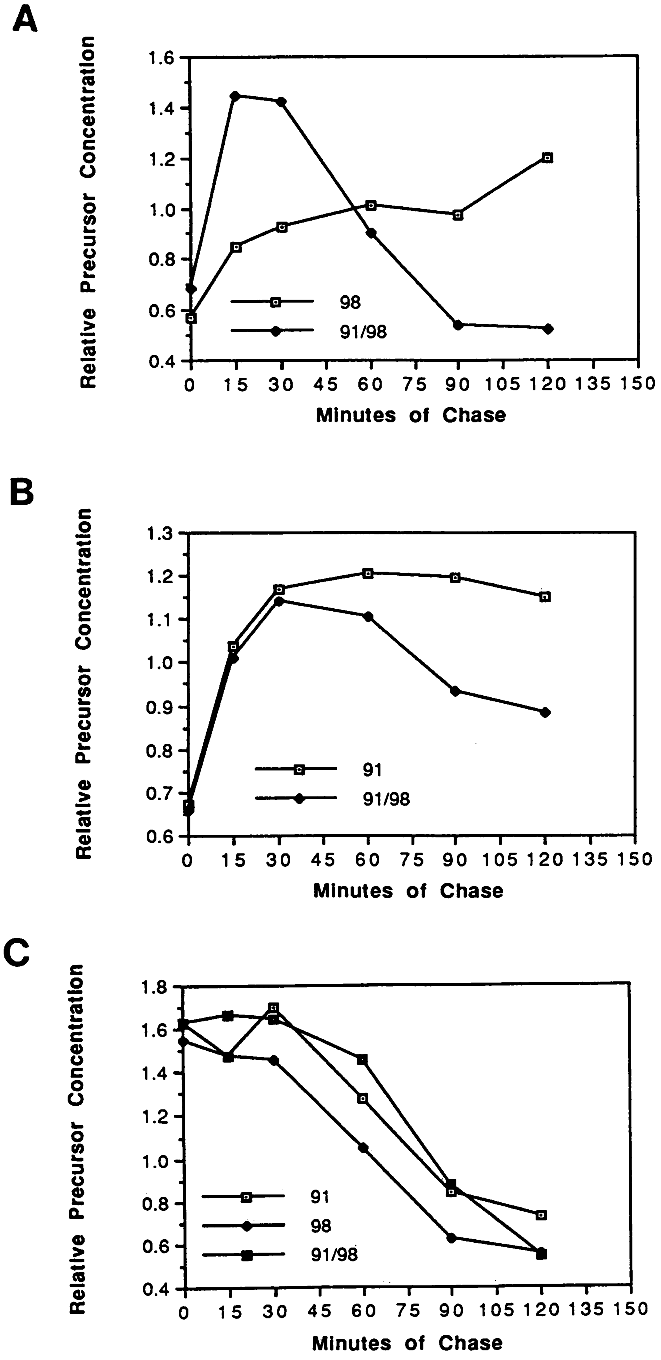

FIG. 7. Quantitative densitometry analysis of the complementation assay. The autoradiographs from Fig. 6 were scanned with an LKB Ultroscan XL laser densitometer. The graphs depict the chase kinetics of each precursor glycoprotein as measured by its disappearance. (A) Taken from the data in Fig. 6A; (B) taken from the data in Fig. 6B; (C) taken from the data in Fig. 6C.

which the pulse-labeled proteins should be a mixture of both ER- and Golgi-modified proteins. Finally, a 90-min chase sample was taken to represent matured proteins.

Samples were solubilized in 1% Triton X-100, layered on a 5 to 15% sucrose gradient containing 0.1% Triton X-100, and sedimented at 40,000 rpm in an SW40 rotor at 4°C overnight. No reducing agents were used during the solubilization and sedimentation. Lysis conditions were chosen to minimize nonspecific aggregation. After sedimentation, the gradient was fractionated, and the samples were immunoprecipitated with either the gI monoclonal antibodies or the polyvalent gp63 precursor-specific antiserum Rb1544.

The first experiment was to identify the monomeric species of precursor and mature forms of each glycoprotein. This was done by disrupting the complex with a combination of SDS and heat. In experiments not shown, we had determined that only SDS and heat treatments of extracts were required to prevent coimmunoprecipitation. A 60-min chase point was taken, and the cells were lysed as described in Materials and Methods and either untreated (to identify complexes) or treated with 1% SDS at 65°C for 10 min (to disrupt complexes releasing the monomers). After the treatment, the samples were loaded onto a 5 to 15% sucrose gradient containing only 0.1% Triton X-100 or 0.1% Triton X-100 plus 0.1% SDS. The gradients were sedimented at 40,000 rpm in an SW40 rotor for 20 h at 4°C. At this time, the samples were fractionated and each fraction divided in two portions. One portion was immunoprecipitated with the pool of gI monoclonal antibodies. The other portion was immunoprecipitated with a gp63-specific polyclonal antibody that reacts with both precursor and mature forms (Rb1544+). From previous experiments, we knew that these antibodies would recognize all forms of SDS-denatured gI and gp63 proteins (data not shown). The results of this experiment are shown in Fig. 8; the left side of each panel corresponds to the bottom of the gradient, and the right side corresponds to the top of the gradient.

Figure 8A shows the untreated lysate immunoprecipitated with the pool of gI antibodies. All forms of gI as well as gp63 were observed in fractions 9 to 11, which defines the position of the gI-gp63 complex. Figure 8C shows that this complex could be completely dissociated by treatment with 1% SDS at 65°C. After SDS and heat treatment, the pool of gI antibodies now immunoprecipitated gI only, presumably because gp63 is no longer complexed to gI. Furthermore, after SDS and heat treatment, the gI protein sedimented significantly more slowly (in fractions 12 and 13) than did gI found in the untreated lysate. These species of gI are presumably the gI monomers. The resolution of the gradient is noteworthy since we consistently observed a separation of the gI monomer precursor and the monomeric mature form. Fraction 12 contained the mature form of the gI, while fraction 13 was enriched for gI monomeric precursors.

Analysis of these same fractions with the anti-gp63 serum is shown in Fig. 8B and D. The complex of gI and gp63 was immunoprecipitated from untreated samples (Fig. 8B) and sedimented in fractions 10 and 11. After treatment with SDS and heat, the gI-gp63 complex was apparently dissociated, because no form of gI was immunoprecipitated with the anti-gp63 serum and the majority of the gp63 species sedimented more slowly than did the original complex (Fig. 8D, fractions 13 and 14). The more slowly sedimenting forms of gp63 presumably represented the gp63 monomers. After treatment with SDS, antiserum Rb1544+ reacted weakly with the mature form of gp63, enabling us to identify both precursor and mature forms of gp63 in the gradient. Unexpectedly, a fraction of the gp63 precursor (not the gp63 mature form or any gI species) was present from fraction 16 to the bottom of the gradient. This was not a technical error, since each gradient fraction was divided in two portions and immunoprecipitated with either the pool of gI antibodies or the gp63 antibody. This result suggested that a significant

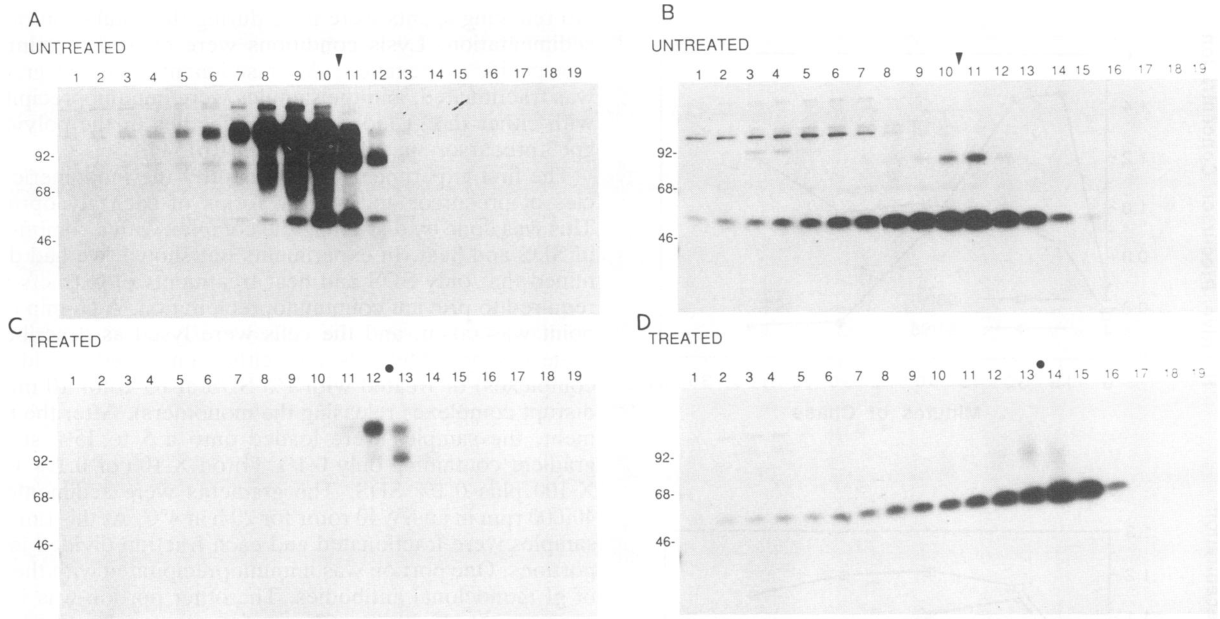

FIG. 8. Gradient fractionation of untreated and SDS-treated gI-gp63 complex. The cells were pulse-labeled as described for Fig. 7. The samples were chased for 60 min and then solubilized as described in legend to Fig. 7 and Materials and Methods. Half of the samples were left untreated (A and B), and half were treated with 1% SDS at 65°C for 10 min (C and D). After the treatment, the samples were sedimented through a 5 to 15% sucrose gradient containing 0.1% Triton X-100. Treated samples were sedimented in gradients containing 0.1% Triton X-100 and 0.1% SDS. The fractions were immunoprecipitated with either a pool of gI monoclonal antibodies (A and C) or the gp63-specific Rb1544+ (B and D). The immunoprecipitates were resolved on an SDS-polyacrylamide gel and visualized by fluorography. The left of each panel corresponds to the bottom of the gradient, and the right corresponds to the top of the gradient. Positions of molecular mass standards (in kilodaltons) are indicated at the left of each panel. The relative positions of the complex of gI and gp63 and the monomers of gI and gp63 are indicated at the top of each panel by an arrow and a dot, respectively.

amount of gp63 precursor was not processed to the mature species, did not assemble properly, and formed aggregates with aberrant sedimentation properties.

As judged from cosedimentation of marker proteins and the gII homodimer complex (44), the complex sedimented as predicted for a heterodimer of gI and gp63 (fractions 10 and 11). Any combination of trimers or tetramers would have sedimented faster than the gII complex.

In the second part of these experiments, we determined the kinetics of oligomer formation (Fig. 9). In this protocol, we took samples at the earliest time possible after a 2-min pulse when we could identify gI proteins with our antisera (Fig. 9A). We also took a 90-min chase sample to examine efficiency of complex formation (Fig. 9C). The immunoprecipitations with the gI monoclonal antibody are shown in Fig. 9A. The critical observation is that we could see complexes at the earliest time point, after 10 min of chase. The gI antibody coprecipitated precursors of both gI and gp63 in predominantly two fractions (fractions 11 and 12). These precursors sedimented faster than predicted for either monomer, which would sediment in fractions 14 and 15.

The 90-min chase time with the gI monoclonal antibody demonstrated that no gI or gp63 reactive protein sedimented further down the gradient, suggesting that no higher oligomers were formed. In addition, at 90 min, mature, processed species were present in the same gradient fractions as observed for the 10-min chase point and also in the next fraction (fraction 10). It is important to note that few precursors sediment in this fraction and that the mature forms sedimenting as monomers were never observed. Thus, not only did gI and gp63 form a complex, but oligomerization was rapid and occurred before significant glycoprotein processing was observed. It is likely that complex formation happens in the ER soon after cotranslational addition of high-mannose sugars. In contrast, PRV glycoprotein gII requires a significant amount of time to form homodimers in the ER (44). We infer from these results that after complex formation in the ER, the gI-gp63 oligomer was transported to the Golgi, where final processing occurred.

Analysis with antiserum 1544 (gp63 precursor specific) provided significant insight into the oligomerization process (Fig. 9B and D). After 10 min of chase, we detected a significant quantity of more slowly sedimenting gp63 precursor in fraction 14 (corresponding to gp63 monomers). However, the antiserum also identified a population of oligomeric gp63, as indicated in fractions 11 and 12. At 90 min after the pulse, antiserum Rb1544 identified a population of gI-gp63 oligomers lacking mature modifications. We speculate that since these oligomers lacked Golgi modifications, they were still within the ER.

DISCUSSION

When the rat retina is infected with the virulent strain PRV-Be, the virus moves from the ganglion cells in the retina along the optic nerve to retinorecipient regions of the forebrain and midbrain (6). The attenuated strain PRV-Ba infects the retina but is largely confined to areas of the brain involved in regulation of the circadian rhythms (6). This striking restricted neurotropism phenotype was mapped to a large deletion in the unique short region of PRV-Ba that removed several genes (23, 30, 45). A single gene responsible

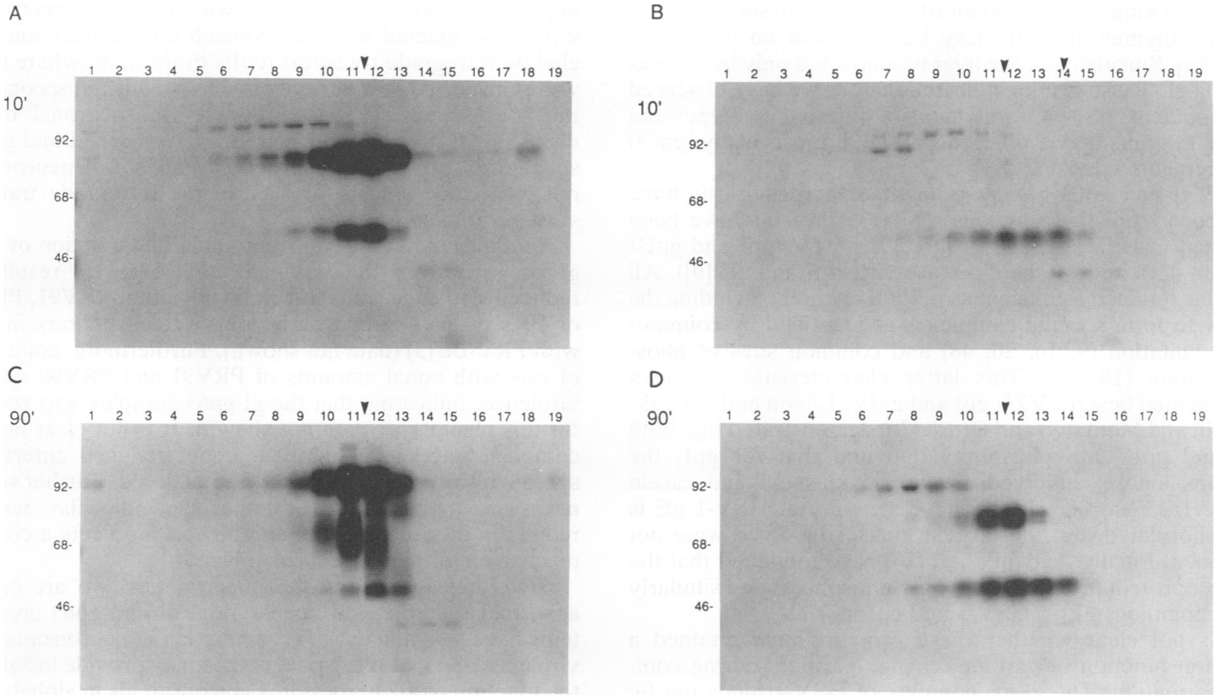

FIG. 9. Gradient fractionation of gI and gp63. PK15 cells were infected at an MOI of 10. The cells were pulse-labeled as described in Materials and Methods at 6 h postinfection and chased for 10 (A and B) and 90 (C and D). The cells were solubilized in 1% Triton X-100 and fractionated by sedimentation through a 5 to 15% sucrose gradient containing 0.1% Triton X-100 at 40,000 rpm for 20 h at 4°C. The fractions were immunoprecipitated with either gI monoclonal antibody 1/14 (A and C) or gp63-specific antiserum Rb1544 (B and D). The immunoprecipitates were resolved on an SDS-polyacrylamide gel and visualized by fluorography. The left of each panel corresponds to the bottom of the gradient, and the right corresponds to the top of the gradient. Positions of molecular mass standards (in kilodaltons) are indicated at the left of each panel. The relative position of the gI-gp63 complex is indicated by the arrowhead at the top of each panel.

for this phenotype was subsequently identified by making defined deletions in the virulent PRV-Be strain. In this way, it was shown that PRV91, which lacks only the gI gene, had the restricted neurotropism phenotype (5). Card et al. noted that while gI was necessary for infection of the visual circuits of the rat, it might not be sufficient (5). This notion followed from observations of Zuckermann et al. (48), who suggested that gI could be immunoprecipitated with gp63, another PRV glycoprotein also encoded in the unique short region of the PRV genome. Their work implied that a complex of gI and gp63 might be important for function. Since transport of PRV to the rat visual circuits required gI, this paradigm offered an excellent opportunity to determine whether gp63 played any role in this process.

We first constructed precise deletions of gI and gp63 in the virulent PRV-Be strain and demonstrated that absence of either gI, gp63, or both converted the retinal circuit neurotropism from the extensive PRV-Be pattern to the restrictive PRV-Ba pattern. This observation is consistent with the idea that gI and gp63 function as a complex in retinal circuit neurotropism. While further work is necessary to prove this idea in neurons of an intact animal, we were able to corroborate and extend the observations of Zuckermann et al. (48) that gI and gp63 form oligomers in infected cells. This interaction occurred rapidly after synthesis in the ER and was maintained as the glycoproteins traveled through the export pathway even into the mature virus particle. The glycoprotein complex was stabilized by noncovalent interactions, most probably hydrophobic interactions. For example, the gI-gp63 complex could be disrupted by both SDS and heat, while dithiothreitol had no effect, indicating that disulfide bonds did not play a role in complex formation. In contrast, disulfide bonds are required for stabilization of the PRV gII homodimer (44). Significantly, complementation experiments demonstrated that the interactions between these glycoproteins were required for efficient conversion of precursor to mature species and that complex formation was required for efficient transport of these proteins from the ER to the Golgi.

Interestingly, absence of either gI or gp63 had little effect on virus growth in cultured PK15 cells, as determined by single-step growth curves (data not shown). These experiments demonstrated no difference in the rate of formation, the rate of release, or the overall accumulation of infectious virus in PK15 cells. Similar observations were also reported by Mettenleiter et al. (26), who searched for a function of the gI glycoprotein by analyzing the growth and virus release in a variety of cell types. They observed no apparent growth disadvantages to viruses which lack gI and gp63 in PK15 cells but noted that lack of gI slightly inhibited release of virus from rabbit kidney cells. A more significant release defect in these cells was observed when both gI and gIII were deleted (47). It is noteworthy that the presence of gI was deleterious to virus growth in chicken embryo fibroblast cells. Passage of virus in this cell type resulted in rapid selection of deletions removing gI and gp63 (25). Kovacs and Mettenleiter (18) noted that gI affected the organotropism in intranasally infected mice. In these studies, viruses expressing the gI glycoprotein were able to infect a variety of tissues with the notable exception of liver. In mice infected by viruses lacking gI, the amount of virus in all tissues was less but the thymus and olfactory bulb showed no detectable infection. Surprisingly, the liver was infected only by viruses lacking gI. These results indicated that, as we have observed in the intact CNS, PRV infections of different cell types and organ systems have different gI (and most likely gp63) requirements.

The gI and gp63 homologs in other herpesviruses have also been studied. Homologs for these proteins have been reported in HSV (gE and gI [16, 17]), VZV (gpI and gpIV [20, 30, 46]), and Marek's disease virus (gI and gE [9]). All proteins retained significant structural features, including the ability to form specific complexes as identified by coimmunoprecipitation (9, 16, 20, 48) and common sites of phosphorylation (10, 30). This latter characteristic has been documented best for VZV gpI and gpIV. Litwin and coworkers (20) and Montalvo and Grose (30) demonstrated that both gpI and gpIV are phosphorylated and that for gpI, the proteins kinases involved are casein kinase I and casein kinase II. Edson et al. (10) have shown that HSV-1 gE is phosphorylated, but the protein kinases involved were not identified. Finally, Litwin et al. (20) have predicted that the gI glycoprotein of PRV is probably phosphorylated similarly to its homologs gE in HSV-1 and gpI in VZV.

It is not clear whether these proteins have retained a common function or can interchange partners during complex formation. The gI-gE complex of HSV-1 binds the Fc portion of human immunoglobulin (16, 17, 36). This binding is thought to occur directly through gE and is enhanced by the presence of gI (17). The VZV gpI-gpIV complex has similar properties. The Fc region of human immunoglobulin is bound directly to gpI, and the binding is enhanced by gpIV (20). The affinity of binding of the VZV complex to immunoglobulin is significantly lower than that of the HSV-1 or HSV-2 gI-gE complex. The homologs in PRV and Marek's disease virus do not appear to bind the Fc region of human immunoglobulin (9, 48). Both complexes, however, have been reported to be important in virulence (3, 5, 9, 22, 27, 28, 33).

The experiments in tissue culture, mice, and chicken embryos demonstrated that phenotypes for gI and gp63 could be found only in certain cell types. The experiments described here clearly demonstrate that this is also true for infection of the rat visual system. It is clear that both gI and gp63 are required only for infection of specific classes of neurons in the visual centers of the brain (the dorsal and ventral geniculate nuclei and the optic tectum). To infect these areas of the CNS, the virus must infect cells in the retina, travel in an anterograde fashion through axons in the optic nerve, exit the axon at or near synaptic contacts with postsynaptic neurons, and finally enter these neurons and replicate. We suggest that the gI-gp63 complex is important for one of the steps required to reach the visual centers involved in visual discrimination and reflexes but not centers of the brain involved in the regulation of circadian functions. Previously we speculated that the step at which the complex was most likely required was entry into the retinal ganglion cells. It is just as likely, however, that the complex is required for anterograde transport through the specific axons that project to the visual centers of the brain. Alternatively, the final step of crossing the synapse may be the point at which the complex is required. At this time, we have no evidence to support or refute any of these possibilities.

The neurotropism phenotype in infection of retinal circuits is particularly remarkable in that we observe no requirement for gI or gp63 for infection of the visceral neuraxis defined by vagus innervation (data not shown). In these experiments, virus was injected into the stomach musculature and traveled by retrograde transport to the brain stem, where it then was transported to a variety of well-established second- and third-order neurons via retrograde transneuronal mechanisms (4). It may be that the requirement for gI and gp63 is specific for anterograde spread in a subset of neurons and not retrograde spread (at least in the retrograde transport systems studied to date).

Another noteworthy observation is that deletion of either gI or gp63 from the virulent strain PRV-Be resulted in reduced virulence. Rats infected with either PRV91, PRV98, or PRV99 lived significantly longer than did rats infected with PRV-Be (5) (data not shown). Furthermore, coinfection of rats with equal amounts of PRV91 and PRV98 restored virulence, indicating that the gI-gp63 complex was required for this phenotype (data not shown). It is not clear how the complex functions in virulence, but reduced anterograde spread in some neurons must be considered. Further work is necessary to understand whether the molecular basis for reduction of virulence and neurotropism reflects a common mechanism or separate mechanisms.

Nevertheless, despite the uncertainties, we are encouraged that the so-called nonessential gI and gp63 glycoproteins have a significant in vivo function in neurotropism and virulence and that these phenotypes may provide insight into the function of the herpesvirus glycoproteins in alphaherpesvirus pathogenesis.

ACKNOWLEDGMENTS

Henry Pautler provided expert technical assistance. We gratefully acknowledge the help and advice of Jeff O'Brian, Raymond Meade, and Logan House.

REFERENCES

1. **Bartha, A.** 1961. Experimental reduction of virulence of Aujeszky's disease virus. Magy. Allatorv. Lapja **16:**42–45.
2. **Ben-Porat, T., and A. S. Kaplan.** 1985. Molecular biology of pseudorabies virus, p. 105–173. *In* B. Roizman (ed.), The herpesviruses. Plenum Publishing Corp., New York.
3. **Berns, A., A. Van Den Ouweland, W. Quint, J. van Oirschot, and A. Gielkens.** 1985. Presence of markers for virulence in the unique short region or repeat region or both of pseudorabies hybrid viruses. J. Virol. **53:**89–93.
4. **Card, J. P., L. Rinaman, J. S. Schwaber, R. R. Miselis, M. E. Whealy, A. K. Robbins, and L. W. Enquist.** 1990. Neurotropic properties of pseudorabies virus: uptake and transneuronal passage in the rat central nervous system. J. Neurosci. **10:**1974–1994.
5. **Card, J. P., M. E. Whealy, A. K. Robbins, and L. W. Enquist.** 1992. Pseudorabies virus envelope glycoprotein gI influences both neurotropism and virulence during infection of the rat visual system. J. Virol. **66:**3032–3041.
6. **Card, J. P., M. E. Whealy, A. K. Robbins, R. Y. Moore, and L. W. Enquist.** 1991. Two alphaherpesvirus strains are transported differentially in the rodent visual system. Neuron **6:**957–969.
7. **Carlin, B. E., and J. P. Merlie.** 1986. Assembly of multisubunit membrane proteins, p. 71–86. *In* A. W. Strauss, I. Boume, and G. Kreil (ed.), Protein compartmentalization. Springer-Verlag, New York.
8. **Chamberlain, J. P.** 1979. Fluorographic detection of radioactivity in polyacrylamide gels with the water soluble fluor sodium salicylate. Anal. Biochem. **98:**132–135.
9. **Chen, X., P. Brunovskis, and L. F. Velicer.** Unpublished data.
10. **Edson, C. M., B. A. Hosler, and D. J. Waters.** 1987. Varicella zoster virus gpI and herpes simplex virus gE: phosphorylation

and Fc binding. Virology 161:599–602.

11. **Einfield, D., and E. Hunter.** 1988. Oligomeric structure of a prototype retrovirus glycoprotein. Proc. Natl. Acad. Sci. USA 85:8688–8692.
12. **Fuchs, W. H.-J. Rziha, J. Lukacs, I. Braunschweiger, N. Visser, D. Lutticken, C. Schreurs, H.-J. Thiel, and T. Mettenleiter.** 1990. Pseudorabies virus glycoprotein gI: in vitro and in vivo analysis of immunorelevant epitopes. J. Gen. Virol. 71:1141–1151.
13. **Gething, M. J., K. Millammon, and J. Sambrook.** 1986. Expression of the wild type and mutant forms of influenza hemagglutinin: the role of folding in intracellular transport. Cell 46:939–950.
14. **Hampl, H., T. Ben-Porat, L. Ehrlicher, K. O. Habermehl, and A. S. Kaplan.** 1984. Characterization of the envelope proteins of pseudorabies virus. J. Virol. 52:583–590.
15. **Jansen, A. S. P., G. J. Ter Horst, T. C. Mettenleiter, and A. D. Loewy.** 1992. CNS cell groups projecting to the submandibular parasympathetic preganglionic neurons in the rat: a retrograde transneuronal viral cell body labeling study. Brain Res. 572:253–260.
16. **Johnson, D. C., and V. Feenstra.** 1987. Identification of a novel herpes simplex virus type 1-induced glycoprotein which complexes with gE and binds immunoglobulin. J. Virol. 61:2208–2216.
17. **Johnson, D. C., M. C. Frame, M. W. Ligas, A. M. Cross, and N. D. Stow.** 1988. Herpes simplex virus immunoglobulin G Fc receptor activity depends on a complex of two viral glycoproteins, gE and gI. J. Virol. 62:1347–1354.
18. **Kovacs, F., and T. C. Mettenleiter.** 1991. Firefly luciferase as a marker for herpesvirus (pseudorabies virus) replication *in vitro* and *in vivo*. J. Gen. Virol. 72:2999–3008.
19. **Kreis, T. E., and H. F. Lodish.** 1986. Oligomerization is essential for transport of vesicular stomatitis virus glycoprotein to the cell surface. Cell 46:929–937.
20. **Litwin, V., W. Jackson, and C. Grose.** 1992. Receptor properties of two varicella-zoster virus glycoproteins, gpI and gpIV, homologous to herpes simplex virus gE and gI. J. Virol. 66:3643–3651.
21. **Lomniczi, B., L. M. Blankenship, and T. Ben-Porat.** 1984. Deletions in the genome of pseudorabies virus vaccine strains and existence of four isomers of the genome. J. Virol. 49:970–979.
22. **Lomniczi, B., S. Watanabe, T. Ben-Porat, and A. S. Kaplan.** 1984. Genetic basis of the neurovirulence of pseudorabies virus. J. Virol. 52:198–205.
23. **Lomniczi, B., S. Watanabe, T. Ben-Porat, and A. S. Kaplan.** 1987. Genome location and identification of functions defective in the Bartha vaccine strain of pseudorabies virus. J. Virol. 61:796–801.
24. **Lukacs, N., H.-J. Thiel, T. Mettenleiter, and H.-J. Rziha.** 1985. Demonstration of three major species of pseudorabies virus glycoproteins and identification of a disulfide-linked glycoprotein complex. J. Virol. 53:166–173.
25. **Martin, X., and M. Dolivo.** 1983. Neuronal and transneuronal tracing in the trigeminal system of the rat using herpes virus suis. Brain Res. 273:253–276.
26. **Mettenleiter, T. C., B. Lomniczi, N. Sugg, C. Schreurs, and T. Ben-Porat.** 1988. Host cell-specific growth advantage of pseudorabies virus with a deletion in the genome sequences encoding a structural glycoprotein. J. Virol. 62:12–19.
27. **Mettenleiter, T. C., N. Lukacs, A. S. Kaplan, T. Ben-Porat, and B. Lomniczi.** 1987. Role of a structural glycoprotein of pseudorabies virus in virus virulence. J. Virol. 61:4030–4032.
28. **Mettenleiter, T. C., N. Lukacs, and H.-J. Rziha.** 1985. Mapping of the structural gene of pseudorabies virus glycoprotein A and identification of two nonglycosylated precursor polypeptides. J. Virol. 53:52–57.
29. **Mettenleiter, T. C., N. Lukacs, and H.-J. Rziha.** 1985. Pseudorabies virus avirulent strains fail to express a major glycoprotein. J. Virol. 56:307–311.
30. **Montalvo, E. A., and C. Grose.** 1986. Varicella zoster virus glycoprotein gpI is selectively phosphorylated by a virus-induced protein kinase. Proc. Natl. Acad. Sci. USA 83:8967–8971.
31. **Nadelhaft, I., P. L. Vera, J. P. Card, and R. R. Miselis.** 1992. Central nervous system neurons labeled following the injection of pseudorabies virus into the rat urinary bladder. Neurosci. Lett. 143:271–274.
32. **Petrovskis, E. A., J. G. Timmins, T. M. Gierman, and L. E. Post.** 1986. Deletions in vaccine strains of pseudorabies virus and their effect on synthesis of glycoprotein gp63. J. Virol. 60:1166–1169.
33. **Quint, W., A. Gielkens, J. Van Oirshot, A. Berns, and H. T. Cuypers.** 1987. Construction and characterization of deletion mutants of pseudorabies virus: a new generation of live vaccines. J. Gen. Virol. 68:523–534.
34. **Robbins, A. K., J. P. Ryan, M. E. Whealy, and L. W. Enquist.** 1989. The gene encoding the gIII envelope protein of pseudorabies virus vaccine strain Bartha contains a mutation affecting protein localization. J. Virol. 63:250–258.
35. **Roizman, B.** 1990. Herpesviridae: a brief introduction, p. 1787–1793. *In* B. N. Fields et al. (ed.), Virology. Raven Press, Ltd., New York.
36. **Roizman, B., and A. Sears.** 1990. Herpes simplex viruses and their replication, p. 1795–1841. *In* B. N. Fields et al. (ed.), Virology. Raven Press, Ltd., New York.
37. **Rotto-Percelay, D. M., J. G. Wheeler, F. A. Osorio, K. B. Platt, and A. D. Loewy.** 1992. Transneuronal labeling of spinal interneurons and sympathetic preganglionic neurons after pseudorabies virus injections in the rat medial gastrocnemius muscle. Brain Res. 574:291–306.
38. **Rouiller, E. M., M. Capt, M. Dolivo, and F. DeRibaupierre.** 1986. Tensor tympani reflex pathways studied with retrograde horseradish peroxidase and transneuronal viral tracing techniques. Neurosci. Lett. 72:247–242.
39. **Ryan, J. P., M. E. Whealy, A. K. Robbins, and L. W. Enquist.** 1987. Analysis of pseudorabies virus glycoprotein gIII localization and modification by using novel infectious viral mutants carrying unique *Eco*RI sites. J. Virol. 61:2251–2257.
40. **Sarmiento, M., and P. G. Spear.** 1979. Membrane proteins specified by herpes simplex viruses. IV. Conformation of the virion glycoprotein designated VP7(B2). J. Virol. 29:1159–1167.
41. **Sternberger, L. A.** 1979. The unlabeled antibody peroxidase anti-peroxidase (PAP) method, p. 104–169. *In* L. Sternberger (ed.), Immunohistochemistry. John Wiley & Sons, Inc., New York.
42. **Strack, A. M., and A. D. Loewy.** 1990. Pseudorabies virus: a highly specific transneuronal cell body marker in the sympathetic nervous system. J. Neurosci. 10:2139–2147.
43. **Strack, A. M., W. B. Sawyer, J. H. Hughes, K. B. Platt, and A. D. Loewy.** 1989. A general pattern of CNS innervation of the sympathetic outflow demonstrated by transneuronal pseudorabies viral infections. Brain Res. 491:156–162.
44. **Whealy, M. E., A. K. Robbins, and L. W. Enquist.** 1990. The export pathway of the pseudorabies virus gB homolog gII involves oligomer formation in the endoplasmic reticulum and protease processing in the Golgi apparatus. J. Virol. 64:2512–2515.
45. **Wittmann, G., and H.-J. Rziha.** 1989. Aujeszky's disease (pseudorabies) in pigs, p. 230–333. *In* G. Wittmann (ed.), Herpesvirus diseases of cattle, horses, and pigs. Kluwer Academic, Boston.
46. **Yao, Z., W. Jackson, B. Forghani, and C. Grose.** 1993. Varicella-zoster virus glycoprotein gpI/gpIV receptor: expression, complex formation, and antigenicity within the vaccinia virus-T7 RNA polymerase transfection system. J. Virol. 67:305–314.
47. **Zsak, L., T. C. Mettenleiter, N. Sugg, and T. Ben-Porat.** 1989. Release of pseudorabies virus from infected cells is controlled by several viral functions and is modulated by cellular components. J. Virol. 63:5475–5477.
48. **Zuckermann, F., T. C. Mettenleiter, C. Schreurs, N. Sugg, and T. Ben-Porat.** 1988. Complex between glycoproteins gI and gp63 of pseudorabies virus: its effect on virus replication. J. Virol. 62:4622–4626.